

Flexible and degradable resistive switching memory fabricated with sodium alginate

Zhuang-Zhuang Li(李壮壮), Zi-Yang Yan(严梓洋), Jia-Qi Xu(许嘉琪), Xiao-Han Zhang(张晓晗), Jing-Bo Fan(凡井波), Ya Lin(林亚), and Zhong-Qiang Wang(王中强)

Citation: Chin. Phys. B, 2021, 30 (**4**): 047302. DOI: 10.1088/1674-1056/abc67a

Journal homepage: http://cpb.iphy.ac.cn; http://iopscience.iop.org/cpb

What follows is a list of articles you may be interested in

Influence of deep defects on electrical properties of Ni/4H-SiC Schottky diode

Jin-Lan Li(李金岚), Yun Li(李赟), Ling Wang(汪玲), Yue Xu(徐跃), Feng Yan(闫锋), Ping Han(韩平), Xiao-Li Ji(纪小丽)

Chin. Phys. B, 2019, 28 (**2**): 027303. DOI: 10.1088/1674-1056/28/2/027303

Effect of Au/Ni/4H-SiC Schottky junction thermal stability on performance of alpha particle detection

Xin Ye(叶鑫), Xiao-Chuan Xia(夏晓川), Hong-Wei Liang(梁红伟), Zhuo Li(李卓), He-Qiu Zhang(张贺秋), Guo-Tong Du(杜国同), Xing-Zhu Cui(崔兴柱), Xiao-Hua Liang(梁晓华)

Chin. Phys. B, 2018, 27 (**8**): 087304. DOI: 10.1088/1674-1056/27/8/087304

Coexistence of unipolar and bipolar modes in Ag/ZnO/Pt resistive switching memory with oxygen-vacancy and metal-Ag filaments

Han-Lu Ma(马寒露), Zhong-Qiang Wang(王中强), Hai-Yang Xu(徐海阳), Lei Zhang(张磊), Xiao-Ning Zhao(赵晓宁), Man-Shu Han(韩曼舒), Jian-Gang Ma(马剑钢), Yi-Chun Liu(刘益春)

Chin. Phys. B, 2016, 25 (**12**): 127303. DOI: 10.1088/1674-1056/25/12/127303

First-principles study of the formation and electronic structure of a conductive filament in ZnO-based resistive random access memory

Zhao Jing, Dong Jing-Yu, Ren Shu-Xia, Zhang Li-Yong, Zhao Xu, Chen Wei

Chin. Phys. B, 2014, 23 (**12**): 127301. DOI: 10.1088/1674-1056/23/12/127301

Resistive switching characteristics of Ti/ZrO_2/Pt RRAM device

Lei Xiao-Yi, Liu Hong-Xia, Gao Hai-Xia, Yang Ha-Ni, Wang Guo-Ming, Long Shi-Bing, Ma Xiao-Hua, Liu Ming

Chin. Phys. B, 2014, 23 (**11**): 117305. DOI: 10.1088/1674-1056/23/11/117305

Flexible and degradable resistive switching memory fabricated with sodium alginate*

Zhuang-Zhuang Li(李壮壮)[1], Zi-Yang Yan(严梓洋)[1], Jia-Qi Xu(许嘉琪)[1], Xiao-Han Zhang(张晓晗)[1], Jing-Bo Fan(凡井波)[1], Ya Lin(林亚)[1,†], and Zhong-Qiang Wang(王中强)[1,2,‡]

[1] *Department of Physics, Northeast Normal University, Changchun* 130024, *China*

[2] *National Demonstration Center for Experimental Physics Education, Northeast Normal University, Changchun* 130024, *China*

(Received 9 October 2020; revised manuscript received 27 October 2020; accepted manuscript online 31 October 2020)

Transient electronics has attracted interest as an emerging technology to solve electronic-waste problem, due to its physically vanishing ability in solution. Here in this work, we demonstrate a flexible and degradable transient resistive switching (RS) memory device with simple structure of Cu/sodium alginate (SA)/ITO. The device presents excellent RS characteristics as well as high flexibility, including low operating voltage (< 1.5 V) and multilevel RS behavior. No performance degradation occurs after bending the device 50 times. Moreover, our device can be absolutely dissolved in deionized water. The proposed SA-based transient memory device has great potential for the development of green and security memory devices.

Keywords: resistive switching memory, sodium alginate, multilevel resistive switching, transient electronics

PACS: 73.40.Sx, 77.22.Jp, 81.07.–b **DOI:** 10.1088/1674-1056/abc67a

1. Introduction

With the rapid development of consumer electronics, electronic waste has become an urgent environmental problem. Therefore, the development of advanced electronic that can be naturally degraded without affecting the environment is highly desired.[1] Recently, transient electronics has been demonstrated to be an emerging technology for the environmentally friendly electronics and secure storage devices. Especially, natural biomaterials, which are typically biocompatible and biodegradable, have attracted great interest for fabricating implantable, wearable, and green electronic devices. Many biocompatible transient electronic elements have been reported, such as light emitting diodes,[2] transistors,[3] and sensors.[4] As one fundamental component in electronic systems, resistive switching (RS) memory has attracted growing interest because its simple structure, fast switching speed, and excellent scalability.[5–7] The development of transient RS device is highly desirable for secure storage and implantable applications. Recently, several kinds of biomaterials have been proposed to prepare RS devices, such as silk,[8] egg albumen,[9] pectin,[10] and lactose.[11] The advantages of these memory devices are their biodegradability and biocompatibility, which can physically disappear completely when the devices are placed in the water. Therefore, the natural biomaterials show great potentials to demonstrate transient resistance random access memory (RRAM) devices.

Sodium alginate (SA), which is a kind of biomass polysaccharide extracted from the brown algae,[12–14] has been widely used in medicine, food field, and textile industry due to its excellent environmental-friendly, non-toxic and biodegradable characteristics.[15–17] Meanwhile, the SA contains C–O–C and C–O–H, and hydroxyl groups, which is conducive to the migration of metal ions by its interacting with these functional groups.[18,19] Hence, the SA is expected to be used to develop the flexible and degradable transient RS devices. In this work, we fabricate a flexible and degradable RS memory based on the SA. The device exhibits the excellent RS characteristics, including low operating voltages (< 1.5 V) and multilevel RS behaviors. Moreover, it can be dissolved in deionized (DI) water, indicating its potential application in the information security device. The degradation product is non-toxic and harmless, which meets the requirements for environmental protection.

2. Experiment

The SA based RS device with Cu (ITO) as top (bottom) electrode was fabricated through some steps as follows. Firstly, 0.1-g SA powder was dispersed in 10-mL deionized water by mechanically stirring at room temperature to form the homogenous SA solution. Secondly, SA films were spin-

*Project supported by the Fund from the Ministry of Science and Technology of China (Grant No. 2018YFE0118300), the National Natural Science Foundation of China (Grant Nos. 11974072, 51902048, 61774031, and 61574031), the "111" Project, China (Grant No. B13013), the China Postdoctoral Science Foundation, China (Grant No. 2019M661185), the Fundamental Research Funds for the Central Universities, China (Grant No. 2412019QD015), and Science Fund from the Jilin Province, China (Grant No. JJKH20201163KJ).

†Corresponding author. E-mail: liny474@nenu.edu.cn

‡Corresponding author. E-mail: wangzq752@nenu.edu.cn

© 2021 Chinese Physical Society and IOP Publishing Ltd

coated on ITO coated polyethylene terephthalate (PET) substrates at room temperature. Finally, 300-μm-diameter Cu top electrodes formed on the SA films each with a shadow mask, by thermal evaporation. The Cu electrode and SA film thickness were determined to be ∼ 30 nm and 20 nm by a step profiler (KLA-Tencor Corporation D-120).

3. Results and discussion

The chemical structure and Fourier-transform infrared (FTIR) spectrum of the as-prepared SA film are shown in Figs. 1(a) and 1(b). The spectrum exhibits the absorption bands at 3462, 1614, 1414, and 1029 cm^{-1}, corresponding to the O–H stretching vibration, COO– stretching vibration, carbonyl (CQO) stretching vibration, and C–O–C stretching vibration, respectively.[20,21] The presence of hydrophilic groups (especially the carboxylic groups) enables SA films to become water soluble, which conduce to the demonstration of transient RS devices. Figures 1(c) and 1(d) show the conceptual schematic diagram and the photograph of flexible Cu/SA/ITO memory device on a PET substrate, respectively. During the electrical measurement, the direction of current flowing from Cu electrode (TE) to ITO electrode (BE) is defined as the positive direction. Figures 1(e) and 1(f) show the atomic force microscopy (AFM) height images of an ITO surface without and with the SA layer. After spin-coated SA layer, the surface roughness value (Ra) of the ITO surface increases slightly from 2.18 nm to 4.65 nm, suggesting the excellent film uniformity of SA films.

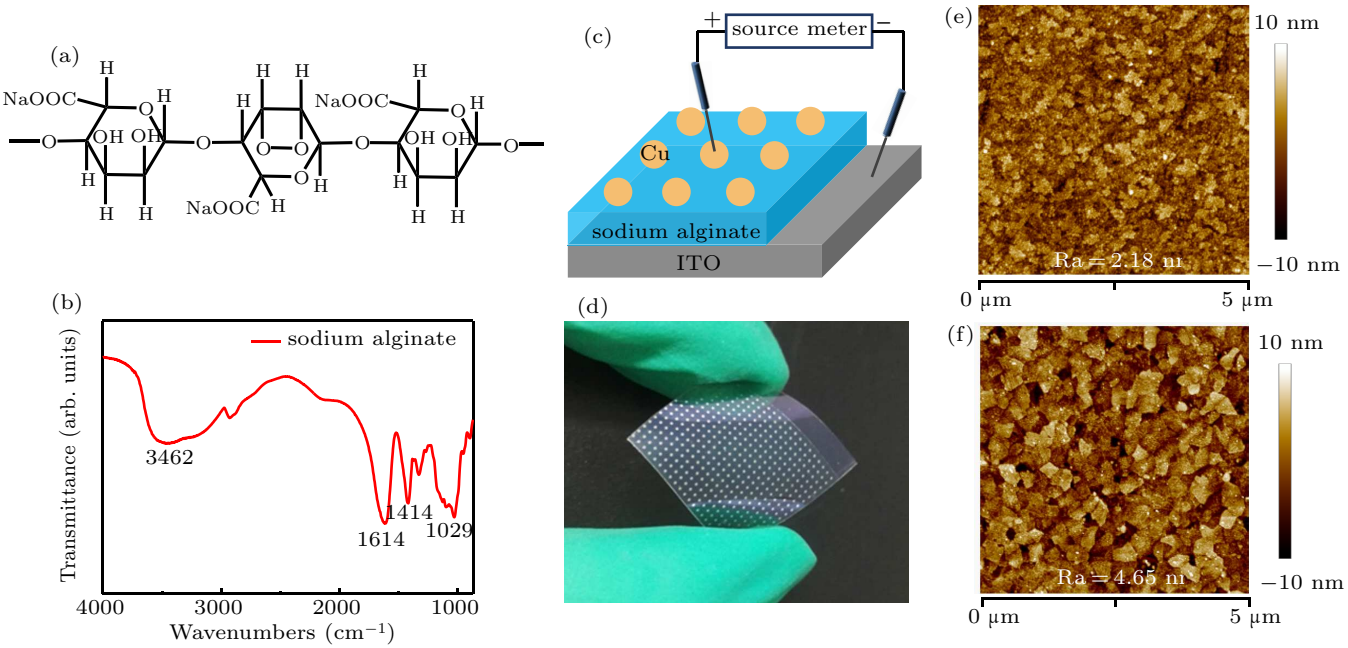


Fig. 1. (a) Chemical structure and (b) FTIR spectrum of SA film. (c) Conceptual schematic diagram and (d) photograph of flexible Cu/SA/ITO memory device on PET substrates. AFM height images of ITO electrode (e) without and (f) with a spin-coated SA layer.

Figure 2(a) shows the typical *I*–*V* curves of Cu/SA/ITO memory cell with a bipolar RS behavior. Herein, a compliance current (CC) of 1 mA is used to protect the devices from being broken down. During positive voltage sweeping from 0 V to 1.5 V, the current increases suddenly at a set voltage (V_{Set}) of ∼ 0.75 V, leading to the transition from high resistance state (HRS) to low resistance state (LRS). Conversely, when the negative voltage sweeps from 0 V to −1.5 V, the current drops abruptly at the reset voltage (V_{Reset}) of ∼ −0.3 V, thus indicating the transition from the LRS to the HRS. Figures 2(b) and 2(c) demonstrate the statistics of resistance and switching voltage during 50 cycles, respectively. As shown in Fig. 2(b), the ON/OFF ratio of the Cu/SA/ITO memory cell reaches 10, facilitating the peripheral circuits to identify the state stored in the device. In Fig. 2(c), the V_{Set} is distributed between 0.25 V and 1.5 V, and the V_{Reset} is distributed between −0.1 V and −1.0 V. The above cumulative probability results show acceptable distributions, indicating the good uniformity. In addition to regenerating RS properties, the cell also displays multilevel RS by controlling CCs of 1 mA and 0.2 mA (red and blue curves) as shown in Fig. 2(d). Obviously, the reproducible RS measurements in Fig. 2(e) show that two distinguishing LRS can be obtained by controlling the values of CC.

Furthermore, the data retention of the multilevel resistance states is shown in Fig. 2(f). We measure three different resistance states under a constant read voltage of 1 mV, and the resistance states exhibit no obvious degradation over 1500 s, indicating the good date retention of Cu/SA/ITO memory.

The conduction mechanism of the Cu/SA/ITO device is analyzed through redrawing the *I*–*V* plot in a log–log scale. As shown in Fig. 3(a), the *I*–*V* curve of LRS presents lin-

ear behavior with a slope close to 1, indicating that it obeys Ohm's law. On the other hand, the conduction behavior of HRS can be divided into two parts: the low voltage bias region (0 V→ 0.5 V) with a slope of about 1 exhibits an Ohmic conductivity characteristic. With the voltage increasing to a relatively high value (from 0.5 V to 0.75 V), the slop is close to 2, which indicates the transport of charge carriers obeys Child's law[22]

$$J_{\text{Child}} = \frac{9}{8}\mu\varepsilon\frac{V^2}{d^3}, \tag{1}$$

where J is the current density, ε is the permittivity of dielectric layer, μ is the mobility of charge carrier, V is the applied voltage, and d is the distance between TE and BE. It demonstrates an indication of trap-controlled space charge limited conduction in this region.[23–25] The trap site may contribute to the defects in the film preparation process, or to the functional groups of the film.[26] Further, a possible RS model can be proposed as shown in Fig. 3(b), in which the formation and rupture of conductive filaments (CFs) can account for the switching between HRS and LRS. When positive voltage is applied to the initial state, the redox reaction of Cu occurs and induces Cu migration into the SA layer in the SET process. Once the Cu CFs link the TE and BE, the device switches from HRS to LRS. When the polarity of the applied voltage is reversed, the electrochemical dissolution of Cu takes place near the ITO, which will reset the device to HRS.

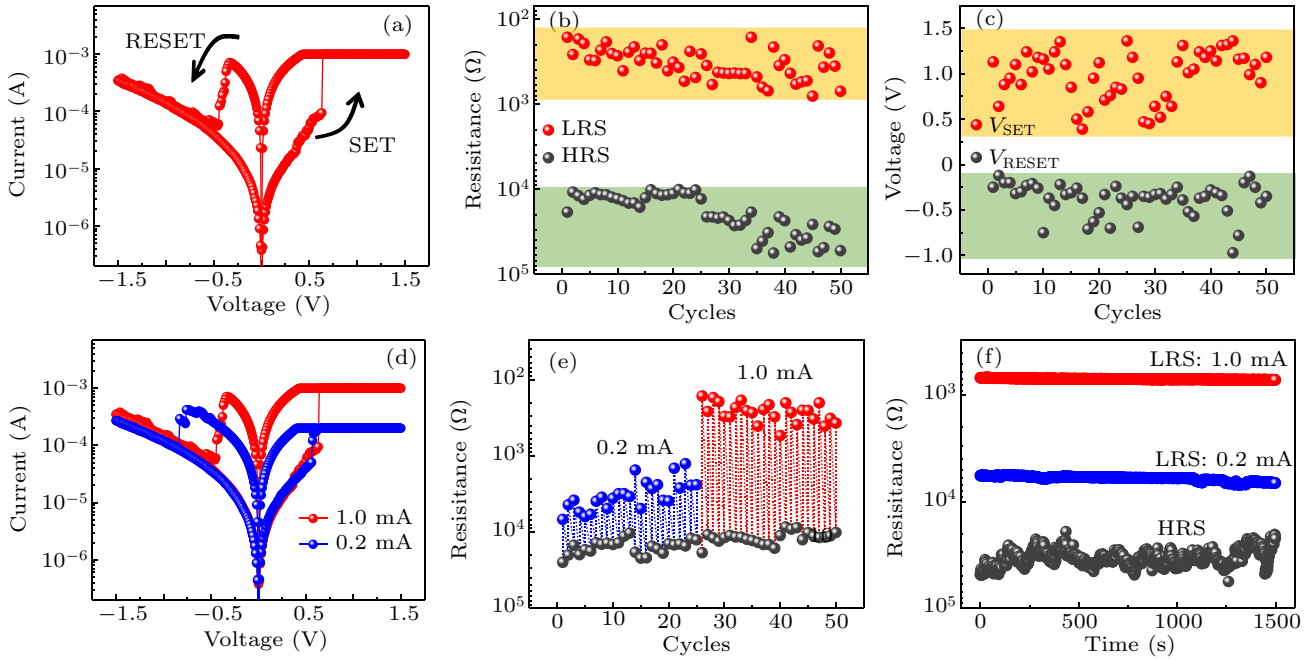


Fig. 2. (a) The *I*–*V* characteristics of the Cu/SA/ITO device. Statistical data on (b) resistance states and (c) switching voltages of 50 switching cycles. (d) Typical *I*–*V* curves of the Cu/SA/ITO device under compliant currents of 1 mA and 0.2 mA (red and blue lines). (e) Statistical data and (f) the retention characteristics of multilevel resistance state.

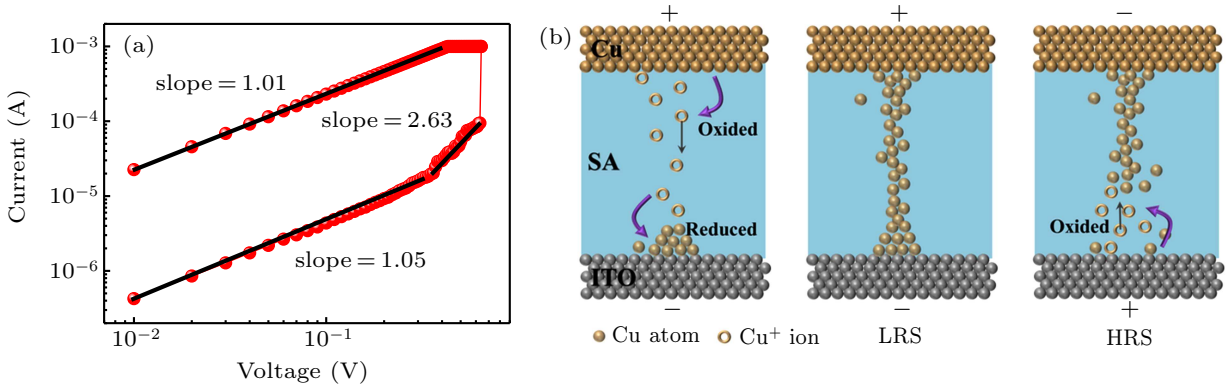


Fig. 3. (a) The log–log scaled *I*–*V* curve of Cu/SA/ITO device, and (b) schematic diagrams for switching mechanism of Cu/SA/ITO device.

The use of organic biomaterials as RS layer in this work enables the device to maintain excellent flexibility. The *I*–*V* curves of our Cu/SA/ITO on PET substrates under flat and bending conditions are shown in Fig. 4(a). Here, the device is placed on the outer surface of a cylinder with a curvature radius as shown in the insert of Fig. 4(a). The same memory behaviors can be obtained before and after bending. Moreover, neither the HRS/LRS nor $V_{\text{Set}}/V_{\text{Reset}}$ has significant degradation after repeated 50 bending cycles as shown in Fig. 4(b). The above results demonstrate that no obvious degradation can

be induced by the mechanical bending, confirming the excellent bending stability of our device and potential application for flexible and wearable electronics.

In order to confirm the transient behavior, the water soluble properties of Cu/SA/ITO memory device are studied. Here, we immerse the fabricated devices in DI water at room temperature. Figure 5 shows a set of evolution images collected in the dissolution process of our memory devices. After being immersed in DI water, the devices gradually disappear due to the dissolution of SA film. It can be seen that our device is dissolved completely after 4.5 h in DI water. With the disappearance of electrodes, the structure of the device is destroyed. Figures 5(g) and 5(h) show the RS behaviors of Cu/SA/ITO device before and after the dissolution process, respectively. It can be seen that the typical RS behaviors disappear after placing the device in DI water for 4.5 h, which further suggests the dissolution of our device. The above results indicate that the Cu/SA/ITO memory is potentially suitable for the development of biodegradable electronics and secure storage device.

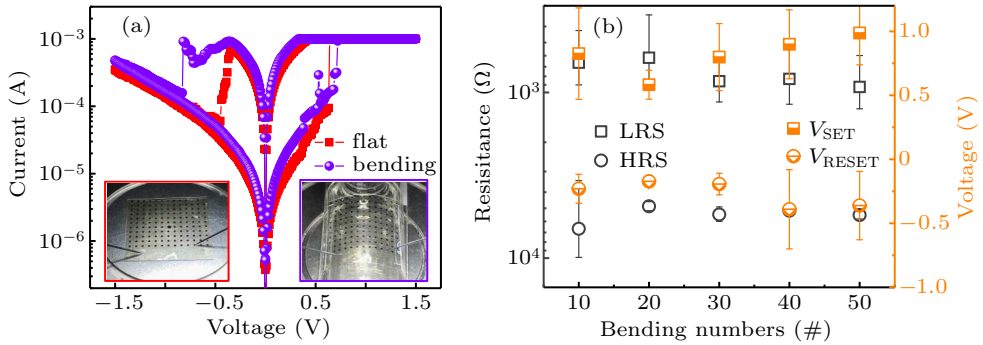


Fig. 4. (a) Comparison among typical *I*–*V* curves in bending test, with inset showing schematically device under electrical measurements; (b) average values of HRS/LRS (V_{SET}/V_{RESET}) under different bending times.

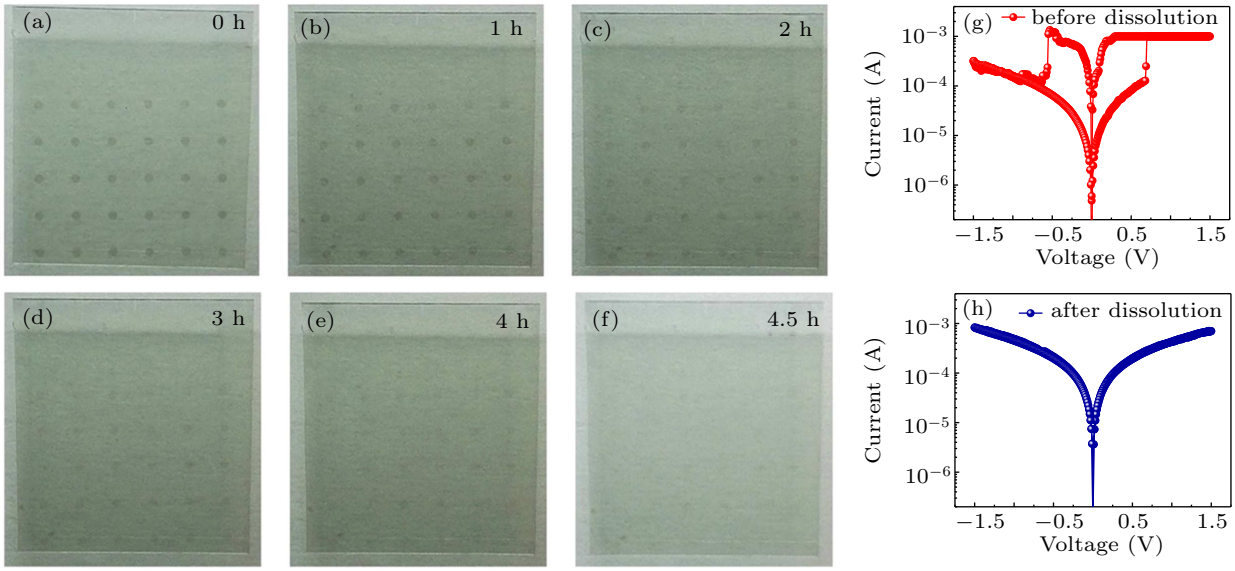


Fig. 5. (a)–(f) Images showing dissolution process of Cu/SA/ITO device in DI water at room temperature, and RS behaviors of Cu/SA/ITO device (g) before and (h) after dissolution process for 4.5 h.

4. Conclusions and perspectives

In this work, we fabricate a Cu/SA/ITO structured flexible and biodegradable resistance switching device, which presents low switching voltage (< 1.5 V) and multilevel RS behavior. The formation and rupture of conducting filaments are assumed to be responsible for the resistive switching behaviors of the device. Our memory device with PET substrate presents excellent flexibility, suggesting potential application in future wearable electronics. Moreover, the device can also disappear after being immersed in DI water for 4.5 h, demonstrating the transient characteristics. This work provides an alternative material for developing the flexible biodegradable resistant switching memory. At the same time, the device degradation product is non-toxic harmless, possessing the function of the green environmental protection of electronic devices. It is expected to become one of the important choices of emerging electronic device.

References

[1] Hwang S, Tao H, Kim D, Cheng H, Song J, Rill E, Brenckle M, Panilaitis B, Won S, Kim Y, Song Y, Yu K, Ameen A, Li R, Su Y, Yang

M, Kaplan D, Zakin M, Slepian M, Huang Y, Omenetto F and Rogers 2012 *Science* **337** 1640
[2] Khanra S, Cipriano T, Lam T, White T A, Fileti E E, Alves W A and Guha S 2015 *Adv. Mater. Interfaces* **2** 1500265
[3] Dai S, Chu Y, Liu D, Cao F, Wu X, Zhou J, Zhou B, Chen Y and Huang J 2018 *Nat. Commun.* **9** 2737
[4] Boutry C M, Beker L, Kaizawa Y, Vassos C, Tran H, Hinckley A C and Bao Z 2019 *Nat. Biomed. Eng.* **3** 47
[5] Yang J, Yang Y, Waltermire S W, Wu X, Zhang H, Gutu T, Jiang Y, Chen Y, Zinn A A, Prasher R, Xu T T and Li D 2011 *Nat. Nanotechnol.* **7** 91
[6] Tao Y, Li X H, Xu H Y, Wang Z Q, Ding W T, Liu W Z, Ma J G and Liu Y C 2018 *IEEE J. Electron Dev.* **6** 714
[7] Shi K X, Xu H Y, Wang Z Q, Zhao X N, Liu W Z, Ma J G and Liu Y C 2017 *Appl. Phys. Lett.* **111** 223505
[8] Wang H, Zhu B W, Ma X H, Hao Y and Chen X D 2016 *Small* **12** 2715
[9] He X L, Zhang J, Wang W B, Xuan W P, Wang X Z, Zhang Q L, Smith C G and Luo J K 2016 *ACS Appl. Mater. Interfaces* **8** 10954
[10] Xu J Q, Zhao X N, Wang Z Q, Xu H Y, Hu J L, Ma J G and Liu Y C 2018 *Small* **15** 1803970
[11] Guo Y Y, Hu W, Zeng F J, Zhang C G, Peng Y and Guo Y C 2020 *Org. Electron.* **83** 105750
[12] Hu W N, Jiang J, Xie D D, Wang S T, Bi K X, Duan H G, Yang J L and He J 2018 *Nanoscale* **10** 14893
[13] Kataoka K, Suzuki Y, Kitada M, Ohnishi K, Suzuki K, Tanihara M, Ide C, Endo K and Nishimura Y and Biomed J 2001 *Mater. Res.* **54** 373
[14] Xia L C, Huang H, Fan Z, Hu D W, Zhang D M, Khan A S, Usman M and Pan L J 2019 *Mater. Design.* **182** 108048
[15] Boppana R, Mohan G K, Nayak U Y, Mutalik S, Sa B and Kulkarni R V 2015 *Int. J. Biol. Macromol.* **75** 133
[16] IIhan E, Cesur S, Guler E, Topal F, Albayrak D, Cuncu M M, Cam M E, Taskin T, Turkoglu H, Sasmazel, Aksu B, Oktar F N and Gunduz O 2020 *Int. J. Biol. Macromol.* **161** 1040
[17] Klekiel T, Mackiewicz A, Pawelska A K, Skonieczna J, Kurowiak J, Piasecki T, Nowak A N and Bedzinski R 2020 *J. Mater. Res. Technol.* **9** 9004
[18] Kim M K and Lee J S 2018 *ACS Nano* **12** 1680
[19] Jumaah F N, Mobarak N N, Ahmad A, Ghani M A and Rahman M Y A 2015 *Ionics* **21** 1311
[20] Wang T, Wang J, Wang R, Yuan P, Fan Z and Yang S 2019 *New J. Chem.* **43** 8684
[21] Wang W, Zhao Y L, Bai H Y, Zhang T T, Ibarra-Galvan V and Song S X 2018 *Carbohydr. Polym.* **198** 518
[22] Chiu F 2014 *Adv. Mater. Sci. Eng.* **2014** 1
[23] Lin Y, Xu H Y, Wang Z Q, Cong T, Liu W Z, Ma H L and Liu Y C 2017 *Appl. Phys. Lett.* **110** 193503
[24] Wang Z Q, Xu H Y, Li X H, Zhang X T, Liu Y X and Liu Y C 2011 *IEEE Electron Dev. Lett.* **32** 1442
[25] Wang W, Xu J Q, Ma H L, Zhao X N, Lin Y, Zhang C, Wang Z Q, Xu H Y and Liu Y C 2018 *ACS Appl. Nano Mater.* **2** 307
[26] Wang H, Meng F B, Cai Y R, Zheng L Y, Li Y G, Liu Y J, Jiang Y Y, Wang X T and Chen X D 2013 *Adv. Mater.* **25** 5498